

Anna Roujeinikova

Manchester Interdisciplinary Biocentre, Faculty
 of Life Sciences, University of Manchester,
 131 Princess Street, Manchester M1 7DN,
 England

Correspondence e-mail:
 anna.roujeinikova@manchester.ac.uk

Received 18 December 2007
 Accepted 25 February 2008

Cloning, purification and preliminary X-ray analysis of the C-terminal domain of *Helicobacter pylori* MotB

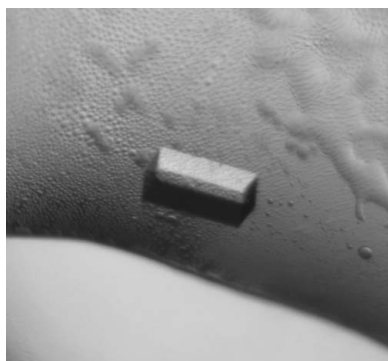
The C-terminal domain of MotB (MotB-C) contains a putative peptidoglycan-binding motif and is believed to anchor the MotA/MotB stator unit of the bacterial flagellar motor to the cell wall. Crystals of *Helicobacter pylori* MotB-C (138 amino-acid residues) were obtained by the hanging-drop vapour-diffusion method using polyethylene glycol as a precipitant. These crystals belong to space group $P2_1$, with unit-cell parameters $a = 50.8$, $b = 89.5$, $c = 66.3$ Å, $\beta = 112.5^\circ$. The crystals diffract X-rays to at least 1.6 Å resolution using a synchrotron-radiation source. Self-rotation function and Matthews coefficient calculations suggest that the asymmetric unit contains one tetramer with 222 point-group symmetry. The anomalous difference Patterson maps calculated for an ytterbium-derivative crystal using diffraction data at a wavelength of 1.38 Å showed significant peaks on the $\nu = 1/2$ Harker section, suggesting that *ab initio* phase information could be derived from the MAD data.

1. Introduction

The bacterial flagellar motor is a molecular machine that rotates helical filaments and allows bacteria to swim toward nutrients, optimal temperatures or other factors that favour survival (DeRosier, 1998). It is embedded in the bacterial cell wall, spanning the outer and inner membranes. The MotA and MotB protein components of the motor form a stator complex that uses the gradient of protons across the cytoplasmic membrane to generate the turning force (torque) applied to the FliG component of the rotor (Manson *et al.*, 1977; Blair & Berg, 1988). MotA has four α -helices that span the cytoplasmic membrane, with the rest of the molecule (about two thirds) forming a cytoplasmic domain (Zhou *et al.*, 1995). MotB is anchored to the cytoplasmic membrane through its N-terminal hydrophobic α -helix, with the bulk of the protein being in the periplasm (Chun & Parkinson, 1988). The sequence of the periplasmic domain of MotB contains a peptidoglycan-binding motif $NX_2LSX_2RAX_2VX_3L$ which is conserved throughout the OmpA family (DeMot & Vanderleydon, 1994). It is therefore thought that the MotA–MotB complex attaches to the cell wall *via* the MotB periplasmic domain.

Helicobacter pylori is a gastric pathogenic bacterium associated with gastric inflammation and peptic ulcers and is a risk factor for gastric cancer (Uemura *et al.*, 2001). A single *motB* gene (No. 0816) has been identified in the *H. pylori* 26695 genome (Tomb *et al.*, 1997). In-frame deletion of the *motB* gene creates flagellated nonmotile *H. pylori* mutants that show a reduced ability to infect mice (Ottemann & Lowenthal, 2002). Motility by the flagellar motor is required during the initial colonization of the stomach (Eaton *et al.*, 1992) and is needed for the bacteria to attain full infection levels (Ottemann & Lowenthal, 2002).

The molecular mechanism of the torque generation by the stator complex remains obscure owing to a lack of structural information for the stator and the rotor–stator interface. A crystallographic approach can be used to investigate the structural basis of peptidoglycan recognition by MotB and to address the possible role of its separate domains in the oligomeric behaviour and assembly of a single stator unit. This paper describes the cloning, overexpression, purification, crystallization and preliminary X-ray diffraction analysis of a putative peptidoglycan-binding domain of *H. pylori* MotB.



2. Materials and methods

2.1. Cloning and overexpression

A sequence-similarity search against the PDB (Berman *et al.*, 2000; <http://www.rcsb.org>) identified two peptidoglycan-binding domains that carry a notable degree of similarity to the periplasmic domain of *H. pylori* MotB. MotB shares 16% sequence identity in a 127-residue overlap with the OmpA-like domain of RmpM from *Neisseria meningitidis* (PDB code 1r1m; Grizot & Buchanan, 2004) and 26% sequence identity in a 102-residue overlap with the periplasmic domain of peptidoglycan-associated lipoprotein from *Escherichia coli* (PDB code 2aiz; Parsons *et al.*, 2006). Domain boundaries for the putative peptidoglycan-binding domain of MotB (MotB-C, comprising the 132 C-terminal residues) were chosen based on the evident conservation of the secondary structures between the three proteins (the MotB secondary structure was predicted using the *JNet* method; Cuff & Barton, 1999).

The coding sequence for MotB-C was PCR-amplified from genomic DNA of strain 26695 of *H. pylori* using KOD Hot Start DNA polymerase (Novagen) and the primers CACCTTTGAAAACGC-TACTTCAGACGCT (forward) and TCATTCTTGCTGTTTGTG-CGGATTG (reverse). The amplified fragment was cloned into the pET151/D-TOPO vector using the TOPO cloning kit (Invitrogen) to produce an expression vector that contains an N-terminal His₆ tag followed by a TEV protease-cleavage site. The expression clone was confirmed by DNA sequencing. The 138-residue recombinant protein used for crystallization comprised residues 125–256 of MotB plus six additional residues from the TEV cleavage site (GIDPFT). The vector was transformed into *E. coli* strain BL21 (Novagen). Cells were grown in LB medium containing 100 mg l⁻¹ ampicillin at 310 K until an OD₆₀₀ of 0.8 was reached, at which point overexpression of MotB-C was induced by adding 1 mM IPTG and growth was continued for a further 3 h. The cells were then harvested by centrifugation at 4500g for 15 min at 277 K.

2.2. Purification

Cells were lysed using the freeze–thaw method followed by sonication in a buffer containing 20 mM sodium phosphate pH 7.4, 100 mM NaCl and 1 mM PMSF. Cell debris was removed by centrifugation at 10 000g for 20 min. NaCl and imidazole were then added to the supernatant to final concentrations of 500 and 10 mM, respectively, after which the supernatant was loaded onto a 5 ml Hi-

Trap Chelating HP column (GE Healthcare) pre-washed with buffer A (20 mM sodium phosphate pH 7.4, 500 mM NaCl, 10 mM imidazole, 1 mM PMSF). The column was washed with 20 column volumes of buffer B (20 mM sodium phosphate pH 7.4, 500 mM NaCl, 80 mM imidazole) and protein was eluted with buffer B containing 500 mM imidazole. The N-terminal tag was cleaved off with His₆-TEV protease (Invitrogen) overnight at 277 K whilst dialysing the sample against buffer C (50 mM Tris–HCl pH 8.0, 0.5 mM EDTA, 2 mM DTT, 200 mM NaCl, 1% glycerol). NaCl and imidazole were then added to the sample to final concentrations of 500 and 10 mM, respectively, and the TEV protease and the uncleaved protein were removed on a Hi-Trap Chelating HP column. The flowthrough was concentrated to 2 ml in a VivaSpin 10 000 Da cutoff concentrator and loaded onto a Superdex 75 HiLoad 26/60 gel-filtration column (GE Healthcare) equilibrated with 50 mM Tris–HCl pH 8.0, 200 mM NaCl. The fractions containing MotB-C were identified using SDS-PAGE, pooled and dialysed overnight against 50 mM Tris–HCl pH 8.0.

2.3. Crystallization and preliminary X-ray analysis

Prior to crystallization, the protein was concentrated to 11 mg ml⁻¹ (based on the Bradford assay; Bradford, 1976) and centrifuged for 20 min at 13 000g to clarify the solution. Initial screening of crystallization conditions was carried out by the hanging-drop vapour-diffusion method using Crystal Screen, Crystal Screen 2 and the PEG/Ion Screen (Hampton Research). Rod-like crystals (Fig. 1) were obtained after 3 d from condition No. 36 of the PEG/Ion Screen, which contained 200 mM sodium tartrate dibasic dihydrate and 20% PEG 3350. This condition was subsequently refined to improve the crystal quality, yielding an optimal composition for the reservoir solution of 100 mM Tris–HCl pH 6.4, 16–18% PEG 3350, 200 mM sodium tartrate. For data collection, crystals were flash-cooled to 100 K after soaking in a cryoprotectant solution equivalent to the

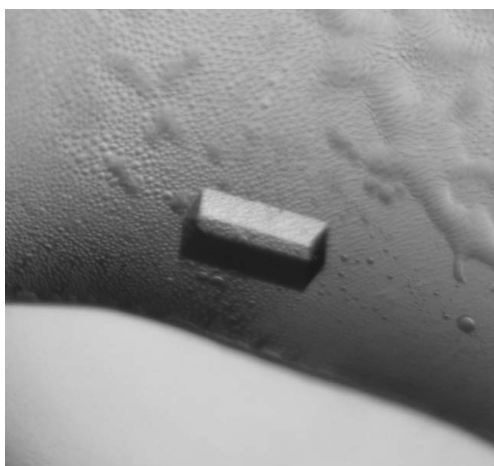


Figure 1
A crystal of *H. pylori* MotB-C.

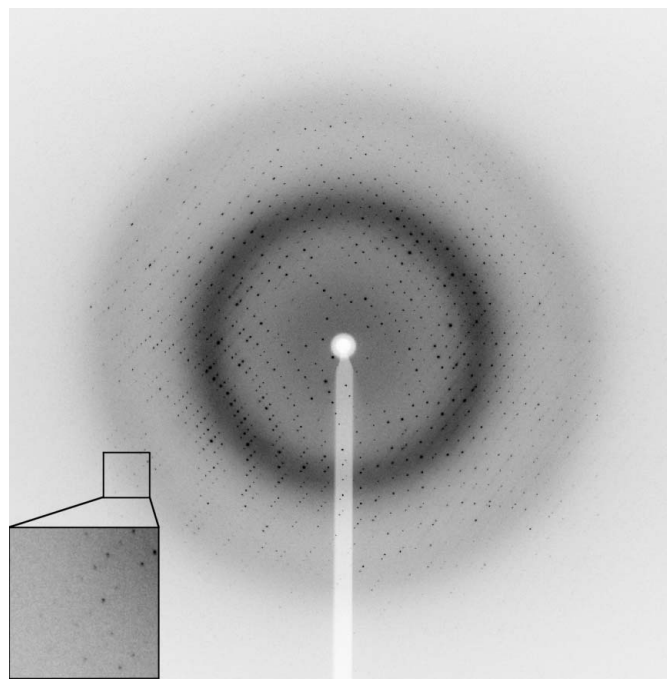


Figure 2
A representative 1° oscillation image of data collected from a native MotB-C crystal using a MAR CCD 225 detector at station PX06, SLS, Switzerland. The magnified rectangle shows diffraction spots at 1.8–1.9 Å resolution.

Table 1

Data-collection statistics.

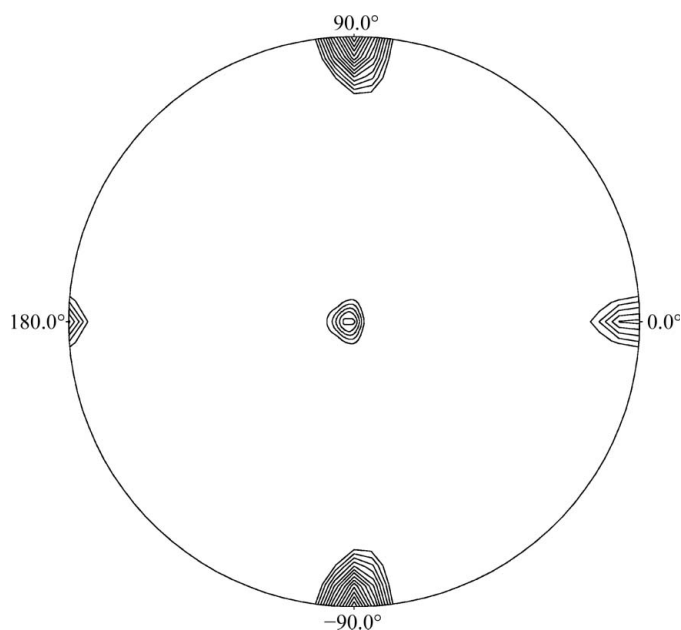
Values in parentheses are for the highest resolution shell.

	Native	Yb peak	Yb inflection	Yb remote
Wavelength (Å)	0.9	1.384	1.386	1.244
Resolution range (Å)	15–1.6	50–2.9	50–2.7	50–2.5
Completeness (%)	99.6 (100.0)	99.7 (100)	98.5 (99.7)	99.1 (99.4)
Observed reflections	270331	41589	50353	64747
Unique reflections	71913	12187	14949	18831
$I/\sigma(I)$	13.1 (2.8)	12.3 (4.0)	11.6 (3.6)	13.3 (3.7)
R_{merge} (%)	7.1 (39.8)	10.8 (30.6)	11.3 (29.6)	9.7 (32.2)

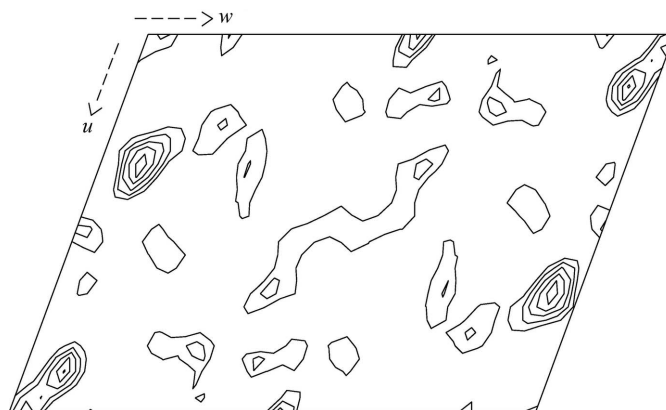
reservoir solution supplemented with 20% (v/v) glycerol. X-ray data were collected from the native crystal to 1.6 Å (Fig. 2) using the Swiss Light Source (PX06, SLS, Villigen, Switzerland). An ytterbium derivative was produced by soaking the native crystal in mother liquor containing 2 mM ytterbium chloride hydrate for 4 h. A multiple-wavelength dispersion (MAD) experiment was performed on a single cryocooled crystal of the ytterbium derivative at 100 K on ESRF beamline BM16 (Grenoble, France). The peak, inflection and remote wavelengths were chosen near the ytterbium absorption edge based on the fluorescence absorption spectrum of the frozen crystal. A total of 180 images were collected at each wavelength using a 1° oscillation width. All data were processed and scaled using the programs *MOSFLM* (Leslie, 1992) and *SCALA* (Collaborative Computational Project, Number 4, 1994). The statistics of data collection are summarized in Table 1.

2.4. Crystallization and preliminary X-ray analysis

Autoindexing of the diffraction data for the native MotB-C crystal using *MOSFLM* showed that the crystals belonged to a primitive monoclinic space group, with unit-cell parameters $a = 50.8$, $b = 89.5$, $c = 66.3$ Å, $\beta = 112^\circ$. Examination of the diffraction patterns using the program *HKLVIEW* (Collaborative Computational Project, Number 4, 1994) showed systematic absences along the $0k0$ axis, with only reflections with $k = 2n$ present, which suggests that the crystals belong


Figure 3

$\kappa = 180^\circ$ section of the self-rotation function. The plot is contoured at levels of 0.75σ starting at 3σ .


Figure 4

Harker section ($0 < u < 1$, $v = 0.5$, $0 < w < 1$) of the anomalous Patterson map for the ytterbium derivative at 5 Å resolution. Contours are drawn at levels of 1σ starting at 1σ .

to space group $P2_1$. Calculations of the Matthews coefficient for three and four molecules in the asymmetric unit gave values of 2.9 and $2.2 \text{ \AA}^3 \text{ Da}^{-1}$, respectively, both of which lie in the range observed for protein crystals (Matthews, 1977). For the self-rotation function, which was calculated using data in the resolution range 12–4.0 Å, no dominant features that could be assigned to noncrystallographic axes were found in the $\kappa = 120^\circ$ section. In contrast, the $\kappa = 180^\circ$ section revealed peaks that correspond to three mutually orthogonal twofold axes, one of which is approximately parallel to the crystallographic b axis (Fig. 3). This suggests that the asymmetric unit contains a tetramer with 222 point-group symmetry.

A three-wavelength MAD experiment has been undertaken on a crystal of MotB-C derivatized with ytterbium chloride hydrate (Table 1). Significant peaks were detected on the $v = 1/2$ Harker section of the anomalous Patterson map calculated at 5 Å resolution (Fig. 4), indicating the presence of two ytterbium ions with similar occupancy. A crystal structure determination based on these data is currently under way.

Genomic DNA of *H. pylori* strain 26695 was a kind gift from Dr Nicola High (University of Manchester). I thank Santina Russo at the Swiss Light Source and Gavin Fox at the European Synchrotron Radiation Facility for assistance with data collection. This work was supported by a Wellcome Trust Research Career Development Fellowship to AR.

References

- Berman, H. M., Westbrook, J., Feng, Z., Gilliland, G., Bhat, T. N., Weissig, H., Shindyalov, I. N. & Bourne, P. E. (2000). *Nucleic Acids Res.* **28**, 235–242.
- Blair, D. F. & Berg, H. C. (1988). *Science*, **242**, 1678–1681.
- Bradford, M. M. (1976). *Anal. Biochem.* **72**, 248–254.
- Chun, S. Y. & Parkinson, J. S. (1988). *Science*, **239**, 276–278.
- Collaborative Computational Project, Number 4 (1994). *Acta Cryst.* **D50**, 760–763.
- Cuff, J. A. & Barton, G. J. (1999). *Proteins*, **40**, 502–511.
- DeMot, R. & Vanderleydon, J. (1994). *Mol. Microbiol.* **12**, 333–334.
- DeRosier, D. J. (1998). *Cell*, **93**, 17–20.
- Eaton, K. A., Morgan, D. R. & Krakowska, S. (1992). *J. Med. Microbiol.* **37**, 123–127.
- Grizot, S. & Buchanan, S. K. (2004). *Mol. Microbiol.* **51**, 1027–1037.
- Leslie, A. G. W. (1992). *Jnt CCP4/ESF-EACBM Newsl. Protein Crystallogr.* **26**.
- Manson, M. D., Tedesco, P., Berg, H. C., Harold, F. M. & Van der Drift, C. (1977). *Proc. Natl Acad. Sci. USA*, **74**, 3060–3064.
- Matthews, B. W. (1977). *The Proteins*, edited by H. Neurath & R. L. Hill, Vol. 3, pp. 468–477. New York: Academic Press.

Ottemann, K. M. & Lowenthal, A. C. (2002). *Infect. Immun.* **70**, 1984–1990.
Parsons, L. M., Lin, F. & Orban, J. (2006). *Biochemistry*, **45**, 2122–2128.
Tomb, J. F. *et al.* (1997). *Nature (London)*, **338**, 539–547.

Uemura, N., Okamoto, S., Yamamoto, S., Matsumura, N., Yamaguchi, S., Yamakido, M., Taniyama, K., Sasaki, N. & Schlemper, R. J. (2001). *N. Engl. J. Med.* **345**, 784–789.
Zhou, J. D., Fazio, R. T. & Blair, D. F. (1995). *J. Mol. Biol.* **251**, 237–242.